Static seismic reliability analysis of SSTF structures

Hui-Juan Liu
Graduate Student, Faculty of Architecture, Civil and Transportation Engineering, Beijing University of Technology, Beijing, China

Yan-Gang Zhao
Professor, Faculty of Architecture, Civil and Transportation Engineering, Beijing University of Technology, Beijing, China

Xuan-Yi Zhang
Associate Professor, Faculty of Architecture, Civil and Transportation Engineering, Beijing University of Technology, Beijing, China

Zhao-Hui Lu
Professor, Faculty of Architecture, Civil and Transportation Engineering, Beijing University of Technology, Beijing, China

ABSTRACT: In order to evaluate the seismic performance of the steel staggered truss framing (SSTF) structural system, the seismic reliability analysis of the structure is carried out in this paper. The limit state function of SSTF structural load bearing capacity was established by taking the total horizontal seismic action at the bottom of the structure reaching the ultimate base shear as the limit state. With the same amount of steel used as the basis, the SSTF structural analysis models were established for the common steel frame structure and six different truss arrangement forms. The failure probabilities of the common steel frame structure model and SSTF structure model under different seismic intensities were calculated using the high-order moment method, and the corresponding failure probability curves were drawn. The results show that: Most of the SSTF structural models have better seismic performance than the common steel frame structural models; Increasing the number of additional members in the truss helps to improve the seismic performance of the SSTF structure; The form of connection between vertical web and chord of the truss affects the seismic performance of the SSTF structure, and the rigid connection is more beneficial than the hinged connection to improve the seismic performance of the SSTF structure.

1. INTRODUCTION

The steel staggered truss framing (SSTF) structure (shown in Figure 1) is a novel kind of steel frame building. When compared to regular steel frame structures, this structure's mechanical qualities and building function are much better thanks to the unusual member arrangement, and it has since emerged as one of the primary steel structure development forms (Gan et al. 2019). The seismic and other safety issues of the structure have received a lot of attention.

At present, the research on the seismic performance of SSTF structures is mainly focused on deterministic analysis（Kim et al. 2015; Zhou et al. 2006). However, in actual engineering, the seismic capacity of structures is affected by a large number of uncertain factors, and deterministic analysis is difficult to truly grasp the seismic performance of structures. Seismic reliability analysis is an important tool to evaluate the seismic performance under different seismic protection levels by considering the influence of random factors (Sun et al. 2020). Unfortunately, the reliability analysis of SSTF structural systems is still a gap. Therefore, it is necessary to carry out the seismic reliability analysis of SSTF structures.

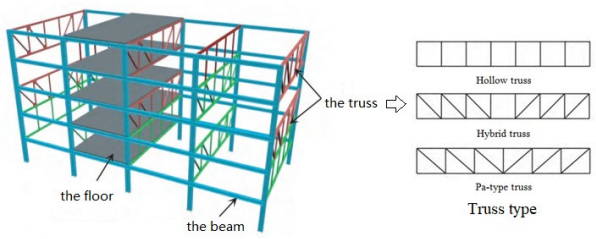

Figure 1: Schematic of SSTF structure.

The commonly used reliability analysis methods are Monte Carlo sampling method, approximate reliability analysis method and high-order moment method (Zhao and Lu 2021). The first two methods have the shortcomings of large computation and repeated iterations to determine the test points. While the higher-order moment method has the advantages of simple and efficient computation and easy integration with finite element analysis techniques, so it is used to carry out the reliability analysis in this paper.

In this paper, the limit state function is established by taking the total horizontal seismic action at the bottom of the structure as the limit state to reach the ultimate base shear. Then, seven numerical analysis models are established for SSTF structure and common steel frame structure. The first four order moments (mean, standard deviation, skewness and kurtosis) of the limit state functions of each structure at different intensity levels are solved by the point estimation method based on one-dimensional dimensionality reduction, and the failure probability is obtained based on the higher order moment method. Finally, the failure probability curves of SSTF structures are constructed by combining the failure probabilities at all intensity levels, and the seismic performance of SSTF structures is studied comparatively.

2. ESTABLISHMENT OF LIMIT STATE FUNCTION OF SSTF STRUCTURE

The seismic design of existing building structures is usually based on the static design method. In order to integrate the safety assessment of SSTF structures with existing design standards and codes. This paper takes the ultimate base shear V_S of the structure as the seismic load carrying capacity of the structure, and the total horizontal seismic action F_E at the bottom of the structure as the seismic action demand of the structure. The limit state function is established as follows.

$$G(\mathbf{X}) = V_S - F_E \tag{1}$$

Under earthquake action, the structure may enter a strong nonlinear state such as damage or collapse, and the analytical calculation of the ultimate basal shear V_S is difficult. Therefore, this paper uses the planar nonlinear analysis software CLAP (Ogawa and Tada 1994) to carry out the structural Pushover analysis to determine the V_S. In earthquake engineering, there are usually five earthquake damage levels of the structure, which need to correspond to four performance levels of the structure, and different performance levels correspond to different limit values of seismic capacity. In this paper, the V_S at different levels is named V_{Si} (i=1,...,4), where V_{S1}, V_{S2}, and V_{S3} are the base shears corresponding to the inter-story displacement angles 1/250, 1/100, and 1/50 on the Pushover curve, respectively, and V_{S4} is the maximum base shear on the Pushover curve. The correspondence between the seismic damage level of the structure and V_{Si} (i=1,...,4) is shown in Table 1.

Table 1: Relationship between seismic and V_{Si} (i=1,...,4)

Damage level	Basically intact	Slightly damaged	Moderately damaged	Severely damaged	Completely damaged
V_S	$V_S<V_{S1}$	$V_{S1}\le V_S<V_{S2}$	$V_{S2}\le V_S<V_{S3}$	$V_{S3}\le V_S<V_{S4}$	$V_S\ge V_{S4}$

In addition, the total horizontal seismic action F_E at the base of the structure based on the single-degree-of-freedom oscillator response spectrum can be expressed in the form of an equivalent static random model in the case of determined site hazards.

$$F_E = ma \tag{2}$$

where m is the equivalent total weight of the structure, and a is the peak acceleration of ground shaking.

The equivalent total weight m of the structure can be simplified as:

$$m = S(D + 0.5L)/g \tag{3}$$

where S is the total area of the structure, D is the constant load per unit area, L is the live load per unit area, and g is the acceleration of gravity.

To calculate the peak ground vibration acceleration a, scholars expressed a as the following equation based on extensive statistical analysis.

$$a = 10^{(I \cdot \lg 2 - 0.1047575)} \tag{4}$$

where I denotes the seismic intensity and is a discrete variable from 1 to 12.

Substituting both Eqs. (3) and (4) into Eq. (2), the total horizontal seismic action at the bottom of the structure can be obtained as:

$$F_{\mathrm{E}} = S(D + 0.5L)/\mathrm{g} \cdot 10^{(I \cdot \lg 2 - 0.1047575)} \tag{5}$$

According to Eqs. (1) and (5), the limit state function of the seismic load capacity of the structure can be obtained as:

$$G(\mathbf{X}) = V_{\mathrm{Si}} - S(D + 0.5L)/\mathrm{g} \cdot 10^{(I \cdot \lg 2 - 0.1047575)}, (i = 1, ..., 4) \tag{6}$$

3. RELIABILITY ANALYSIS METHOD BASED ON HIGHER ORDER MOMENT THEORY

According to the higher-order moment reliability theory, the limit state function can be considered as a random variable obeying a cubic-normal distribution, which in turn yields the fourth-order moment reliability index and failure probability as follows (Zhang et al. 2019).

$$\beta_{4\mathrm{M}} = D_0 P - \frac{1}{D_0} + \frac{a_3}{3a_4}, \; P_f = \Phi(-\beta_{4M}) \tag{7}$$

$$D_0 = \sqrt[3]{2}(\sqrt{q_0^2 + 4p^3} - q_0)^{-\frac{1}{3}}, \; P = \frac{3a_2a_4 - a_3^2}{9a_4^2} \tag{8}$$

$$q_0 = \frac{2a_3^3 - 9a_2a_3a_4 - 27a_4^2(a_2 - \beta_{2M}/k)}{27a_4^3}, \beta_{2M} = \frac{\mu_G}{\sigma_G} \tag{9}$$

$$a_2 = 1 - 3a_4, a_3 = \frac{5 + (35 - \alpha_{3G}^2)a_4^2}{9a_0 + 30 - 0.8\alpha_{3G}^2}\alpha_{3G} \tag{10}$$

$$a_4 = \frac{2a_0}{2a_0 + 46(1 - 1/\alpha_{4G}^2) - \alpha_{3G}^2} \tag{11}$$

$$k = \frac{1}{\sqrt{1 + 2a_3^2 + 6a_4^2}}, a_0 = \frac{\sqrt{3\alpha_{4G} - 4\alpha_{3G}^2 - 5} - 2}{1 - (3\alpha_{3G}^2 + 1)/\alpha_{4G}^2} \tag{12}$$

where μ_G, σ_G, α_{3G}, α_{4G} are the first four order central moments of $G(\mathbf{X})$, i.e., mean, standard deviation, skewness and kurtosis. To improve the computational efficiency, the one-dimensional dimensionality reduction idea is used and $G(\mathbf{X})$ is approximated as:

$$G(\mathrm{X}) \cong \sum_{i=1}^{n}(G_i - G(\boldsymbol{\mu})) + G(\boldsymbol{\mu}) \tag{13}$$

$$G_i(u) = G(\mu_1, \mu_2, ..., \mu_{i-1}, T^{-1}(u), \mu_{i+1}, ..., \mu_n) \tag{14}$$

where $\boldsymbol{\mu}$ is the mean vector, u is a standard normal space random variable, and G_i is only a univariate function of the parameter u_i. Based on Eqs. (13)-(14), the first four order central moments of $G(\mathbf{X})$ can be expressed as (Zhao and Ono 2000).

$$\mu_G = \sum_{i=1}^{n}\mu_{Gi} - (n-1)G(\boldsymbol{\mu}) \tag{15}$$

$$\sigma_G^2 = \sum_{i=1}^{n}\sigma_{Gi}^2 \tag{16}$$

$$\alpha_{3G}\sigma_G^3 = \sum_{i=1}^{n}\alpha_{3Gi}\sigma_{Gi}^3 \tag{17}$$

$$\alpha_{4G}\sigma_G^4 = \sum_{i=1}^{n}\alpha_{4Gi}\sigma_{Gi}^4 + 6\sum_{i=1}^{n-1}\sum_{j>i}^{n}\sigma_{Gi}^2\sigma_{Gj}^2 \tag{18}$$

where μ_{Gi}, σ_{Gi}, α_{3Gi}, α_{4Gi} are the first four order central moments of $G_i(u)$, respectively, calculated as follows Equations.

$$\mu_{G_i} = \sum_{k=1}^{m}\omega_k G_i(u_k) \tag{19}$$

$$\sigma_{G_i}^2 = \sum_{k=1}^{m}\omega_k[G_i(u_k) - \mu_{G_i}]^2 \tag{20}$$

$$\alpha_{3G_i} = \frac{1}{\sigma_{G_i}^3}\sum_{k=1}^{m}P_k[G_i(u_k) - \mu_{G_i}]^3 \tag{21}$$

$$\alpha_{4G_i} = \frac{1}{\sigma_{G_i}^4}\sum_{k=1}^{m}P_k[G_i(u_k) - \mu_{G_i}]^4 \tag{22}$$

where u_k is the kth estimation point and ω_k is the weight of u_k. To balance the computational

efficiency and accuracy, seven-point estimation is used in this paper, and the corresponding u_k and ω_k are shown in Table 2.

Table 2: Estimated point u_k and corresponding weight ω_k

k	1	2	3	4	5	6	7
Estimated points u_k	-3.750	-2.367	-1.1544	0	1.154	2.367	3.750
Weight ω_k	5.483×10^{-4}	3.076×10^{-2}	0.24	0.457	0.24	3.076×10^{-2}	5.483×10^{-4}

4. SEISMIC RELIABILITY ANALYSIS OF TYPICAL SSTF STRUCTURES

4.1. Finite element analysis model of a typical SSTF structure

According to the different forms of truss arrangement, SSTF structure is divided into three types: hollow web, hybrid and Pa type. At the same time, the connection between vertical webs and chords contains two types of rigid and hinged connections. Considering the different combinations of truss arrangement and connection between vertical web and chord, this paper uses CLAP software to build 6 finite element analysis models of SSTF structure with the same steel consumption, taking 5-story steel frame as an example. The names are RT1, RT2, RT3; HT1, HT2, HT3. where "R" (Rigid) means rigid connection between vertical webs and chords, "H" (Hinge) means hinge connection between vertical webs and chords, "T" (Truss) denotes truss, and 1-3 denote hollow web, hybrid and Pa truss arrangement respectively. To carry out a comparative study, a common steel frame structure with the same amount of steel used, named M. The standard floor plan and elevation of each model are shown in Figure 2.

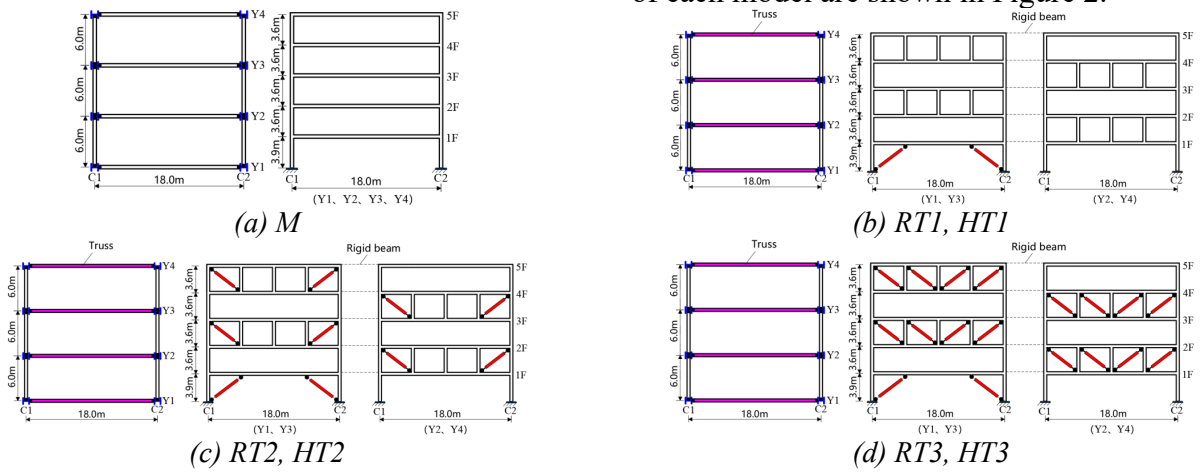

(a) M *(b) RT1, HT1*

(c) RT2, HT2 *(d) RT3, HT3*

Figure 2: Plan and elevations of each structural model

In each model, the longitudinal connecting beams and frame columns are selected from Q355 H-beams, and the webs and chords of trusses are selected from Q235 H-beams, of which the diagonal webs are supported by buckling restrained brace, with material elastic modulus of 205000 N/mm^2 and shear modulus of 79000 N/mm^2. Combined with CLAP analysis software, the steel table is consulted to continuously adjust the beam and column sections of the models, so that the strong column coefficient α_i (Bao et al. 2018) (except for the top floor) is controlled around 2.0 to ensure that the structure is a strong column and weak beam structural system, and finally determine the beam and column dimensions of each model. The cross-sectional dimensions of each model and the strong column coefficients α_i at each level are shown in Table 3.

Table 3: The size of each structural model member

Model	Floor	α_i	Column (Q355)	Beam (Q355)	Vertical web (Q235)	Diagonal webs (Q235)
M	5	1.1	H-492×465×15×20	H-656×301×12×20	/	/
	4	2.2	H-492×465×15×20	H-656×301×12×20		
	3	2.2	H-492×465×15×20	H-656×301×12×20		
	2	2.1	H-502×465×15×25	H-656×301×12×20		
	1	2.3	H-502×465×15×25	H-656×301×12×20		
RT1 HT1	5	1.1	H-400×408×21×21	H-494×302×13×21	H-150×150×7×10	/
	4	2.2	H-400×408×21×21	H-494×302×13×21	H-150×150×7×10	
	3	2.2	H-400×408×21×21	H-494×302×13×21	H-150×150×7×10	
	2	2.1	H-414×405×18×28	H-588×300×12×20	H-150×150×7×10	
	1	2.3	H-414×405×18×28	H-588×300×12×20	/	H-200×200×8×12
RT2 HT2	5	1.1	H-400×408×21×21	H-494×302×13×21	H-125×125×6.5×9	H-100×100×6×8
	4	2.2	H-400×408×21×21	H-494×302×13×21	H-125×125×6.5×9	H-100×100×6×8
	3	2.2	H-400×408×21×21	H-494×302×13×21	H-125×125×6.5×9	H-100×100×6×8
	2	2.1	H-414×405×18×28	H-588×300×12×20	H-125×125×6.5×9	H-100×100×6×8
	1	2.3	H-414×405×18×28	H-588×300×12×20	/	H-200×200×8×12
RT3 HT3	5	1.1	H-400×408×21×21	H-494×302×13×21	H-125×125×6.5×9	H-50×50×6×8
	4	2.2	H-400×408×21×21	H-494×302×13×21	H-125×125×6.5×9	H-50×50×6×8
	3	2.2	H-400×408×21×21	H-494×302×13×21	H-125×125×6.5×9	H-50×50×6×8
	2	2.1	H-414×405×18×28	H-588×300×12×20	H-125×125×6.5×9	H-50×50×6×8
	1	2.3	H-414×405×18×28	H-588×300×12×20	/	H-200×200×8×12

4.2.Identification of random variables

The ultimate base shear of the structure V_{Si} (i=1,...,4) is affected by numerous uncertainties, and the sources of uncertainty can be divided into two categories: material properties of the structure and geometric dimensions of the structure. Since the steel structure itself has a high accuracy of component dimensions, its randomness is much smaller than that of the structural material properties, so only the randomness of the structural material properties is considered in this paper, and the structural geometric dimensions are considered as fixed values for analysis. The statistical information of the random variables associated with the structural material properties is shown in Table 4. The statistical information of the random variables associated with the total horizontal seismic action at the final bottom of the structure, obtained from Eq. (5), is also listed in Table 4.

Table 4: Statistical information of random variables

Random Variables	Distribution	Mean μ_G	Coefficient of variation V_G
Elastic modulus E (kN/cm^2)	Lognormal	2.05×10^4	0.06
Yield strength of beams and columns f_{y1} (kN/cm^2)	Lognormal	3.55×10^1	0.08
Yield strength of vertical and diagonal webs f_{y2} (kN/cm^2)	Lognormal	2.35×10^1	0.08
Second stiffness factor α	Normal	0.01	0.01
Constant load D (kN/m^2)	Normal	6	0.1
Live load L (kN/m^2)	Gamma	2	0.45

4.3 Calculation of the ultimate base shear first fourth-order moment of the structure

In this paper, by combining the point estimation method with the Pushover method (Lv et al. 2010) to solve for V_{Si} (i=1,...,4) for the statistical moment information. The specific steps are as follows.

First, according to Table 4, the random variables affecting V_{Si} (i=1,...,4) of the random variables in Table 4, the estimated points in the original space of the random variables can be obtained by using the 7-point estimates in the standard normal space of Table 1 with the Rosenblatt inverse normal transform. Then, 28 sets of sample points are generated in a one-

dimensional reduced dimensional way, and Pushover analysis is carried out based on each set of sample points to obtain the random Pushover curves.

Finally, based on the four types of limit state values on the random Pushover curves, which are substituted into Eqs. (13)-(22), respectively, the limit states V_{Si} (i=1,...,4) of the first four order moments, as shown in Table 5. For ease of understanding, the 25th set of structural sample points of each model (affecting V_{Si} (i=1,...,4) of the four random variables are taken as the mean values) obtained for the Pushover curves and their corresponding V_{Si} (i=1,...,4) values are plotted in Figure 3.

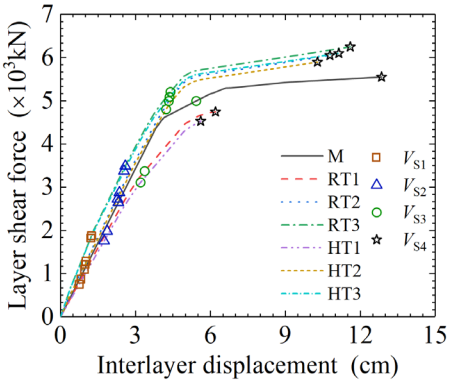

Figure 3: Pushover curves when each model random variable takes the mean value

Table 5: First four central moments of V_{Si} (i=1,...,4) for different structural models

Model	Performance Level	Mean μ_G (kN)	Standard deviation σ_G	Skewness α_{3G}	Kurtosis α_{4G}
M	V_{S1}	1035.33	60.04	0.158	3.04
	V_{S2}	2589.13	150.13	0.158	3.04
	V_{S3}	4938.27	254.59	-0.512	2.72
	V_{S4}	5549.15	417.01	0.217	3.06
RT1	V_{S1}	821.61	48.47	0.147	3.01
	V_{S2}	1991.79	111.27	0.155	3.06
	V_{S3}	3362.88	213.44	-0.106	2.86
	V_{S4}	4704.49	331.14	-0.155	2.78
RT2	V_{S1}	1235.63	82.29	0.116	3.04
	V_{S2}	2860.85	167.16	0.139	3.04
	V_{S3}	4940.03	234.59	-0.192	3.07
	V_{S4}	6027.86	381.91	0.005	3.07
RT3	V_{S1}	1851.89	113.36	0.082	2.9
	V_{S2}	3484.51	177.25	0.09	2.95
	V_{S3}	5216.59	254.73	-0.069	3.11
	V_{S4}	6247.92	376.94	0.186	3.07
HT1	V_{S1}	705.72	42.08	0.165	3.05
	V_{S2}	1764.54	105.33	0.163	3.05
	V_{S3}	3099.2	209.68	-0.148	2.87
	V_{S4}	4478.58	316.46	-0.24	2.91
HT2	V_{S1}	1175.91	82.91	0.049	3.03
	V_{S2}	2724.35	173.28	-0.08	3.34
	V_{S3}	4757.3	251.41	-0.626	4.03
	V_{S4}	5846.05	418.16	-0.393	3.84
HT3	V_{S1}	1802.09	113.58	0.162	3.03
	V_{S2}	3379.18	171.4	0.105	2.95
	V_{S3}	5074.39	246.74	-0.026	3.05
	V_{S4}	6099.17	373.14	0.19	3.07

4.4.Results of seismic reliability analysis of SSTF structures

According to the structural model developed in Section 3.1, the equivalent total weight of the structure can be reduced by combining Eq. (3) as:

$$m = 1.62(D + 0.5L) \tag{23}$$

Substituting Eq. (23) into Eq. (6), the limit state function of the seismic load capacity of this structural model can be obtained as:

$$G(\mathbf{X}) = V_{Si} - 1.62(D + 0.5L) \cdot 10^{(I \cdot \lg 2 - 0.1047575)} \tag{24}$$

where the statistical information of the random variables ultimate base shear V_{Si} (i=1,...,4), constant load D, and live load L are shown in Tables 4 and 5, respectively, and the seismic intensity I is a discrete variable from 1 to 12.

Based on Eq. (24), the first fourth order moments of the limit state function are solved by the one-dimensional reduced dimensional point estimation method, and then the failure probabilities of the structures under different seismic intensities are calculated using Eqs. (7)-(12), and the failure probability curves of the four limit states of each model are shown in Figure 4.

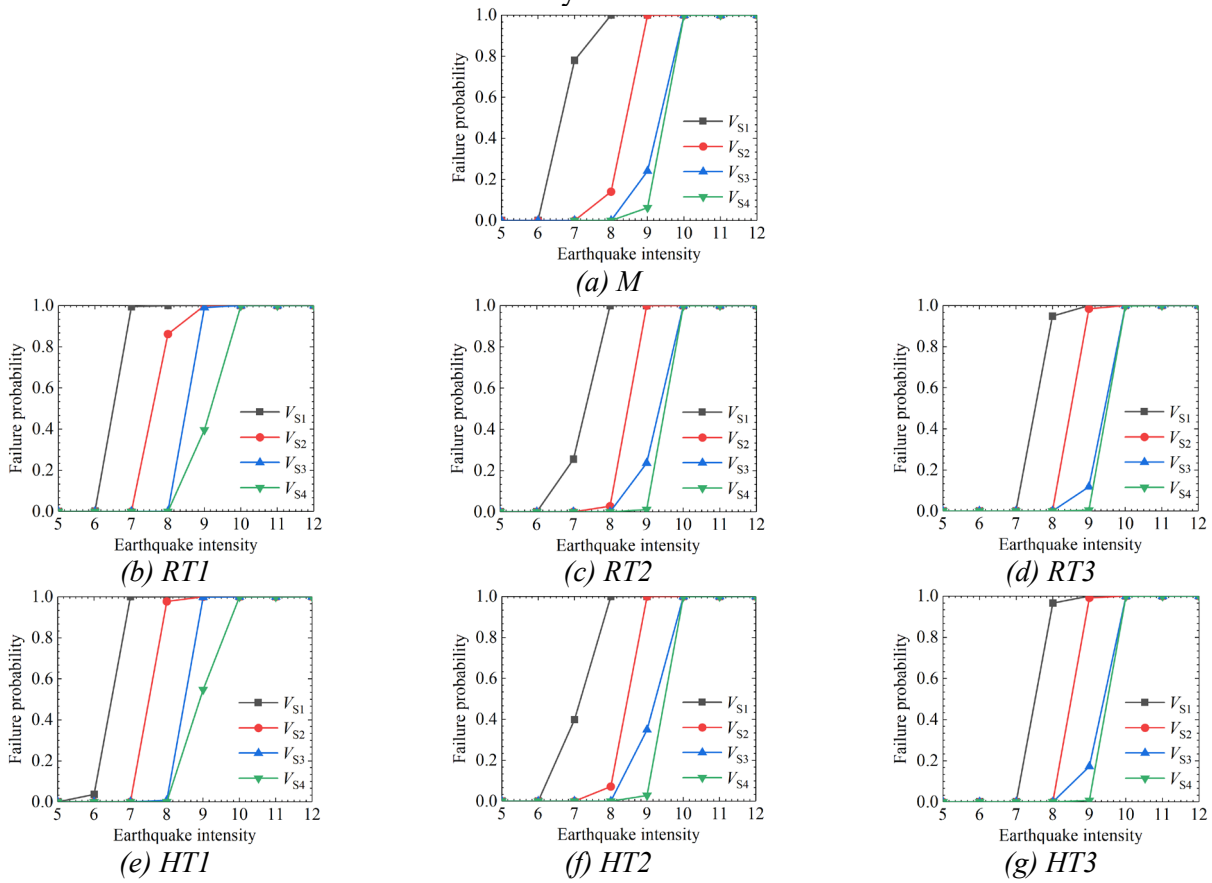

Figure 4: Failure probability curves for each structural model

From Figure 4, it can be seen that.

The failure probability of each structural model increases with the increase of seismic intensity value, and the rate of increase of the failure probability tends to increase first and then decrease.

The failure probability of the same structural model increases with the increase of seismic intensity; the failure probability of V_{S1} corresponding to the performance level is the largest at the same seismic intensity value, and the failure probability of V_{S2}, V_{S3} and V_{S4} corresponding to the performance level decreases in order.

The failure probabilities of different structural models with the same seismic intensity and performance level show a pattern of RT3<HT3<RT2<HT2<M<RT1<HT1. Obviously, except for RT1 and HT1 models, the failure probabilities of all the SSTF structural models are smaller than those of the ordinary steel frame structure M model. This indicates that the hollow web truss form alone is not sufficient to increase the seismic performance of the structure.

In the SSTF structural model, the failure probability of the three types of joist arrangement models shows the pattern of Pa type<hybrid<hollow web under the same seismic

intensity and performance level; the failure probability of the SSTF structural model with rigid connection between vertical web and chord in the joist is less than that of the hinged model under the same joist arrangement model. In order to obtain higher seismic performance, the number of additional members in the joist can be increased and the rigid connection between vertical web and chord is recommended.

5. CONCLUSIONS

In this paper, the seismic reliability analysis of typical SSTF structures under different seismic intensities considering the total horizontal seismic action at the bottom of the structure reaches the ultimate base shear, and the higher-order moment reliability theory is adopted to carry out the seismic reliability analysis considering the uncertainty of structural material parameters. The results help to grasp the variation law of the seismic capacity level of each structural model under different limit states with the seismic intensities. The specific conclusions are as follows.

Compared with ordinary steel frame structures, most SSTF structures have significantly lower probability of failure under the same conditions. Therefore, the SSTF structural model has a better level of seismic capacity among the steel frame structural models with the same amount of steel used.

Different truss arrangement forms have significant effects on the results of seismic reliability analysis of SSTF structures. Among them, the failure probability of Pa-type truss structure is the lowest, and the failure probability of hollow web truss structure is the highest, even higher than the common steel frame structure model. Therefore, the seismic performance of SSTF structure can be improved by increasing the number of additional members (vertical webs and diagonal webs).

In the SSTF structure with the same truss arrangement, the seismic reliability analysis results of the truss vertical webs and chords with rigid and hinged connections are not significantly different, but the overall failure probability shows a trend that the rigid connection is slightly lower than the hinged connection. It can be seen that the rigid connection is better than the hinged one, which is beneficial to improve the overall seismic performance of the structure.

6. REFERENCES

Bao E., Chen Y., Zou C., et al. (2018). “Dynamic performance of low-rise steel frame with exposed steel column base.” Proceedings of the Institution of Civil Engineers-Structures and Buildings, 171(12), 979–991.

Gan D., Zhou X., Zhou Q. (2019). “A review on the seismic behavior of steel staggered truss framing system.” [In Chinese.] *Progress in Steel Building Structures*, 21(4), 1-10.

Kim J., Lee J., Kim B. (2015). “Seismic retrofit schemes for staggered truss structures.” *Engineering Structures*, 102, 93-107.

Lv D., Song P., Yu X., *et al*. (2010). “Nonlinear global seismic reliability analysis of structures based on moment methods.” [In Chinese.] *Journal of Building Structures*, 31(Supp1. 2) ,119-124.

Ogawa K., Tada M. (1994). “Combined non-linear analysis for plane frame (“clap”).” *Architectural Institute of Japan. Proc. of 17th Symposium on Computer Technology on Information Systems and Applications*, Tokyo: Showa intelligence Press, 79-84.

Sun B., Zhang Y., Huang C. (2020). “Machine learning-based seismic fragility analysis of large-scale steel buckling restrained brace frames.” *Computer Modeling in Engineering & Sciences*, 125(2), 755-776.

Zhang X., Zhao Y., Lu Z. (2019). “Unified Hermite polynomial model and its application in estimating non-Gaussian processes.” *Journal of Engineering Mechanics*, 145(3), 04019001.

Zhao Y., Lu Z. (2021). “Structural reliability: approaches from perspectives of statistical moments.” Hoboken: Wiley.

Zhao Y., Ono T. (2000). “New point estimates for probabilistic moments.” *Journal of Engineering Mechanics*, 126(4), 433-436.

Zhou X., Mo T., Liu Y., *et al*. (2006). “Experimental study on high-rise staggered truss steel structure.” [In Chinese.] *Journal of Building Structures*, 27(5), 86-92.